Low temperature Raman and high field ^{57}Fe Mossbauer study of polycrystalline $GaFeO_3$

2010 J. Phys.: Condens. Matter 22 146005

(http://iopscience.iop.org/0953-8984/22/14/146005)

J. Phys.: Condens. Matter **22** (2010) 146005 (6pp) doi:10.1088/0953-8984/22/14/146005

Low temperature Raman and high field ^{57}Fe Mossbauer study of polycrystalline $GaFeO_3$

Kavita Sharma, V Raghavendra Reddy[1], Deepti Kothari, Ajay Gupta, A Banerjee and V G Sathe

UGC-DAE Consortium for Scientific Research, Khandwa Road, Indore-452017, India

E-mail: vrreddy@csr.ernet.in and varimalla@yahoo.com

Received 15 January 2010, in final form 15 February 2010
Published 23 March 2010
Online at stacks.iop.org/JPhysCM/22/146005

Abstract

The magnetic and phonon properties of polycrystalline magnetoelectric/multiferroic $GaFeO_3$ are studied. Using high field ^{57}Fe Mossbauer spectroscopy, occupation of Fe is observed at four cation sites. A Fe population of about 6% is observed at the tetrahedral Ga1 site, which explains the observed pinched-like M–H curve and initial sharp increase of the magnetization. The calculated net magnetization value from Mossbauer data suggests that the Fe moment at the Ga1 site is parallel to Fe1 and opposite to that of Fe2 and Ga2 sites, resulting in ferrimagnetism. From low temperature Raman data, anomalous temperature variation in frequency at T_C is observed for the mode at $\sim$700 cm^{-1}.

(Some figures in this article are in colour only in the electronic version)

1. Introduction

Materials that simultaneously show electric and magnetic ordering are gaining much attention due to their promising multifunctional device applications and because of interesting physics as well [1]. However, for most of the reported multiferroic/magnetoelectric materials the magnetic and ferroelectric transition temperatures are either far lower or far higher than room temperature. For example, some of the materials studied the most in recent years in the context of multiferroic properties, such as $BiMnO_3$ with a Curie temperature (T_C) $\sim$ 105 K, $YbMnO_3$ with T_C $\sim$ 80 K, and $BiFeO_3$ with T_N $\sim$ 643 K [1] etc. As a result the coupling between magnetic and ferroelectric order parameters at room temperature is always weak, which is a major drawback from the application point of view. There have been some efforts to tune magnetic transition temperature close to room temperature, for example in the case of $BiFeO_3$ with about 30% Mn substitution, and hence the possibility of enhanced magnetoelectric coupling at room temperature [2] but with a compromise on the phase purity of the sample. In this context, $GaFeO_3$ (GFO) that exhibits piezoelectricity and ferrimagnetism is considered to be a very promising multiferroic material for the following reasons: (i) its T_C is about 200 K and may be increased to values close to room temperature by increasing the Fe content (x) of $Ga_{2-x}Fe_xO_3$ (T_C $\sim$ 350 K for x = 1.4) or controlling the site disorder between Ga and Fe with different preparation methods [3–5], (ii) it is relatively easy to prepare single phase GFO samples with the conventional solid-state route and (iii) it is considered to be environmentally and biologically friendly when compared to most of the other lead and bismuth based magnetoelectric materials.

GFO was first discovered by Remeika *et al* [5], and its crystallographic properties were described by Abrahams *et al* [6]. GFO crystallizes in an orthorhombic structure with space group $Pc2_1n$ with four different cation sites, namely two Fe^{3+} sites and two Ga^{3+} sites labeled as Fe1 and Fe2 (predominantly occupied by Fe) and A1 and A2 (predominantly occupied by Ga) [6]. Ideal GFO without any site disorder is found to have an antiferromagnetic spin configuration in its ground state. In reality, on the other hand, it is reported to have excess Fe atoms or defects [4] which has complicated the understanding of magnetism in GFO. Recent theoretical and experimental studies on single crystal samples suggest that the excess Fe atoms occupying the octahedral Ga

[1] Author to whom any correspondence should be addressed.

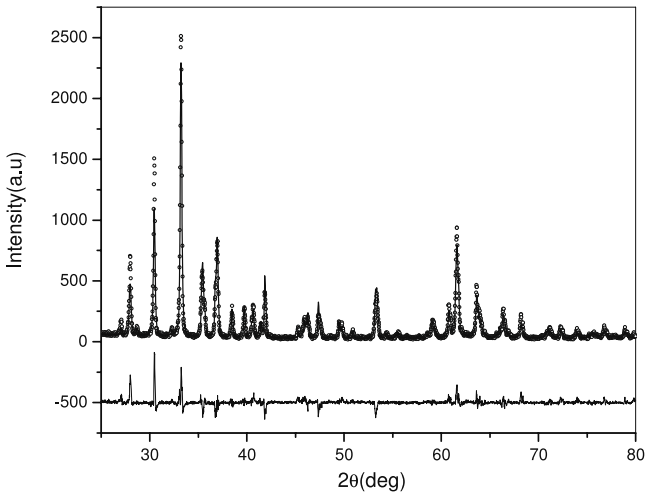

Figure 1. XRD pattern of a $GaFeO_3$ powder sample along with Rietveld refinement.

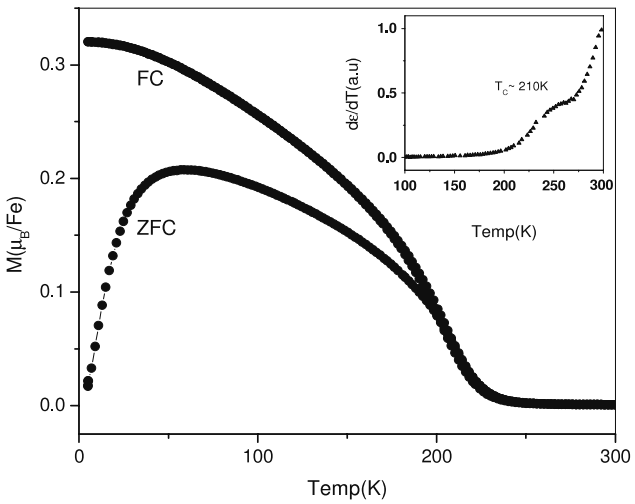

Figure 2. Field cooled (FC) and zero field cooled (ZFC) data measured in a 500 Oe field. The inset shows the variation of the derivative of the dielectric constant with temperature, measured at 100 kHz. Note the anomaly in the dielectric constant data around T_C.

sites are ferromagnetically coupled with the Fe atom at one of the two Fe sites, which results in the net magnetic moments observed in the experiments [4, 7, 8]. Therefore, estimation of cation distribution of Fe in each sublattice is necessary. High field ^{57}Fe Mossbauer spectroscopy, which gives the above information unambiguously, is used in the present work. GFO has also been the focus of several experiments showing interesting properties, such as magnetization induced second-harmonic generation [9], x-ray directional dichroism [10], the optical magnetoelectric effect [11], an unusually large orbital magnetic moment [12] etc, but the behavior of phonons is not reported in the literature for GFO. Recently, a few reports have shown the evidence for spin–phonon coupling in multiferroic materials, signifying the importance of the study of phonons in these materials for a better fundamental understanding of the phenomenon [13, 14]. In the present work we report low temperature Raman spectroscopy and high magnetic field ^{57}Fe Mossbauer spectroscopy measurements on polycrystalline GFO to study the issues of the phonon spectrum and the distribution of Fe in each sublattice and in turn the magnetic properties.

2. Experimental details

Polycrystalline $GaFeO_3$ (GFO) was prepared through a conventional solid-state reaction method [15]. Stoichiometric mixtures of Ga_2O_3 and Fe_2O_3 of purity higher than 99.9% were mixed, ground and pre-calcined at 1173 K and then 1323 K for 12 h. Finally samples were sintered at 1493 K for 12 h [15]. X-ray diffraction (XRD) measurements were carried out using an 18 kW Rigaku machine with 40 kV and 100 mA power settings. Magnetization measurements were carried out using a Quantum Design PPMS-VSM system and low temperature dielectric constant measurements down to 80 K were done using a home made cryostat. ^{57}Fe Mossbauer measurements were performed in transmission mode with a ^{57}Co radioactive source in constant acceleration mode using a standard PC based Mossbauer spectrometer equipped with a Weissel velocity drive. Velocity calibration of the spectrometer was done with a natural iron absorber at room temperature. Low temperature and high magnetic field ^{57}Fe Mossbauer measurements were carried out using a Janis superconducting magnet. For the high magnetic field measurements, the external field was applied parallel to the γ-rays (i.e. longitudinal geometry). Raman spectra were recorded in backscattering geometry with a LABRAM Jobin–Yvon spectrometer. Low temperature Raman measurements (300–80 K) were carried out by using a commercial LINKAM stage in the unpolarized geometry.

3. Results and discussion

Figure 1 shows the x-ray diffraction (XRD) data along with the Rietveld refinement carried out using the DBWS-9411 program. The data were fitted considering the $Pc2_1n$ space group. The obtained structural parameters are $a = 8.773$ (6) Å, $b = 9.426$ (7) Å and $c = 5.102$ (4) Å, which match with the literature and no extra peaks are observed, confirming the single phase of the prepared sample [15]. Figure 2 shows the M–T data measured in a 500 Oe applied magnetic field. For measuring field cooled (FC) and zero field cooled (ZFC) magnetization, the sample was cooled in the absence of a magnetic field to 5 K and then measurements were taken in the presence of an applied magnetic field during warming (called ZFC) and then during cooling in the same field, and the measurements were taken in warming (called FC). The magnetic transition temperature (T_C) obtained as the differential maximum of the M–T curve is at 210 K with a width of about 30–35 K. The inset of figure 2 shows the variation of the derivative of the permittivity as a function of temperature. The observed anomaly close to T_C clearly suggests the magnetoelectric/multiferroic nature of the sample matching with the literature [15, 16]. Naik and Mahendiran observed a magnetodielectric coefficient of -1.8% close to T_C with 60 mT external magnetic field [16]. Figure 3 shows the M–H loop measured at 5 K.

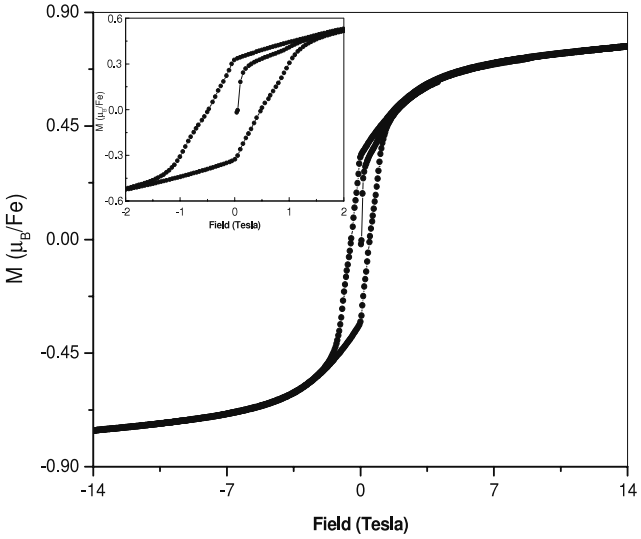

Figure 3. M–H data for a $GaFeO_3$ powder sample measured at 5 K. The inset shows the zoomed part of the same data to highlight the pinched-like hysteresis curve.

The following observations can be made from the magnetization data. (i) The observed hysteresis curve exhibits a pinched-like shape (the zoomed magnetization data are shown in the inset of figure 3 for clarity), which is generally observed in exchange spring magnets because of exchange coupling between hard and soft magnetic phases. In GFO this could also be possible because the four cation sites have different magnetic anisotropy energies, i.e. octahedral sites (Fe1, Fe2 and A2) have strong anisotropy, whereas the tetrahedral A1 site is less anisotropic and hence they act as hard and soft magnetic phases, respectively [4]. The sharp increase followed by a slow increase of the magnetization in the initial magnetization curve is also an indication of the presence of both soft and hard magnetic phases. (ii) Very high magnetic fields are required to saturate, because of high anisotropy of the system. (iii) The observed magnetic moment value from the magnetization data of the present study matches closely with the reported experimental and theoretical value of GFO [3, 4, 7, 12, 16]. (iv) The value of T_C obtained in the present study matches closely with that reported by Sun *et al* [15], but is significantly different from that for ceramic GFO prepared with slow cooling and single crystals of GFO. Even in the case of single crystal samples prepared by different methods, namely float zone and flux methods, the T_C is reported to be different [3–5]. This is mainly attributed to the variation in Fe/Ga site occupations, hence implying that what is magnetically important in this material is the study of cation distributions at the four sites i.e. Fe1, Fe2, A1 and A2.

Figure 4 shows the Mossbauer spectra (MS) recorded at 300, 5 and 5 K, 5 T external magnetic field applied parallel to the γ-rays, i.e. longitudinal geometry. The observed paramagnetic doublet spectrum at 300 K and the magnetic sextet at 5 K are in accordance with the M–T data as shown in figure 2. Soon after the discovery of the magnetoelectric effect in GFO, ^{57}Fe Mossbauer measurements were reported in GFO, and in fact the controversy between ferrimagnetic and

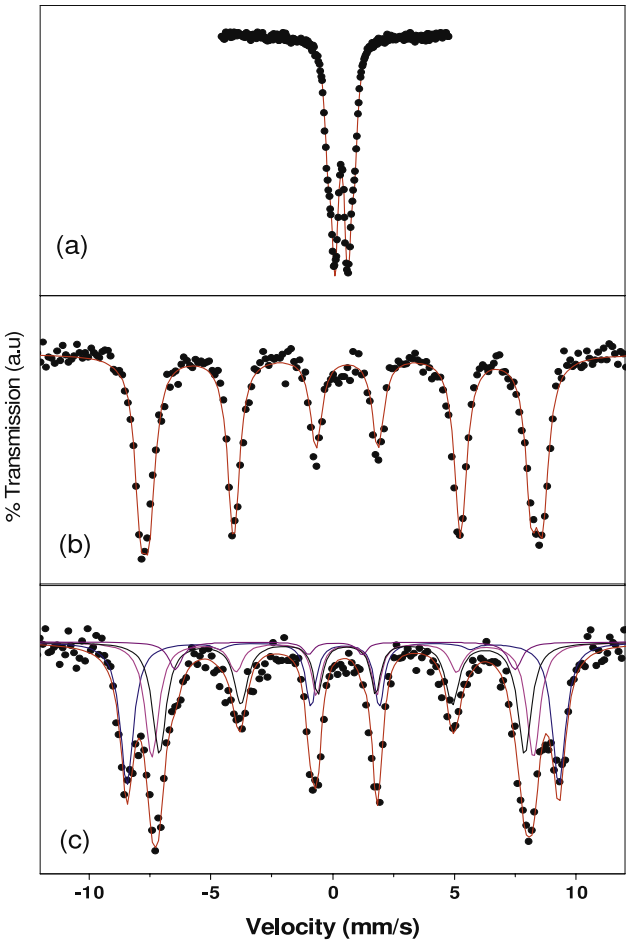

Figure 4. ^{57}Fe Mossbauer spectra at (a) 300 K, (b) 5 K and (c) 5 K and 5 T field applied parallel to the γ-ray beam. The obtained hyperfine parameters from the high field data with respect to natural iron are shown in table 1.

canted antiferromagnetic structure of GFO was resolved with high field Mossbauer data [8, 17]. As mentioned above, since the magnetic properties of GFO vary drastically depending on Fe/Ga site occupation, preparation methods etc, high field MS of the present study is used to estimate cation distribution unambiguously for the polycrystalline sample prepared by the solid-state route. It may be noted that the intensity of the second and fifth lines (which correspond to $\Delta m = 0$ transition lines) is not zero in the high field MS as shown in figure 4(c). This is due to the high magnetic anisotropy of the sample, but not to spin canting [8]. The disappearance of the $\Delta m = 0$ lines depends on the anisotropy of the material. For example, in weakly anisotropic $NiFe_2O_4$ the disappearance occurs at very low fields of the order of 1 T, but for systems with high anisotropy such as GFO the disappearance occurs at very high fields. The high anisotropy of GFO is also evidenced from the observed M–H data (figure 3), which show that fields higher than 14 T are required to saturate.

The observed MS were fitted with the NORMOS-SITE program. The best fit to the data is observed with four sextets. The width of four sextets is constrained to be equal and the A23 parameter, i.e. the area ratio of the second and third

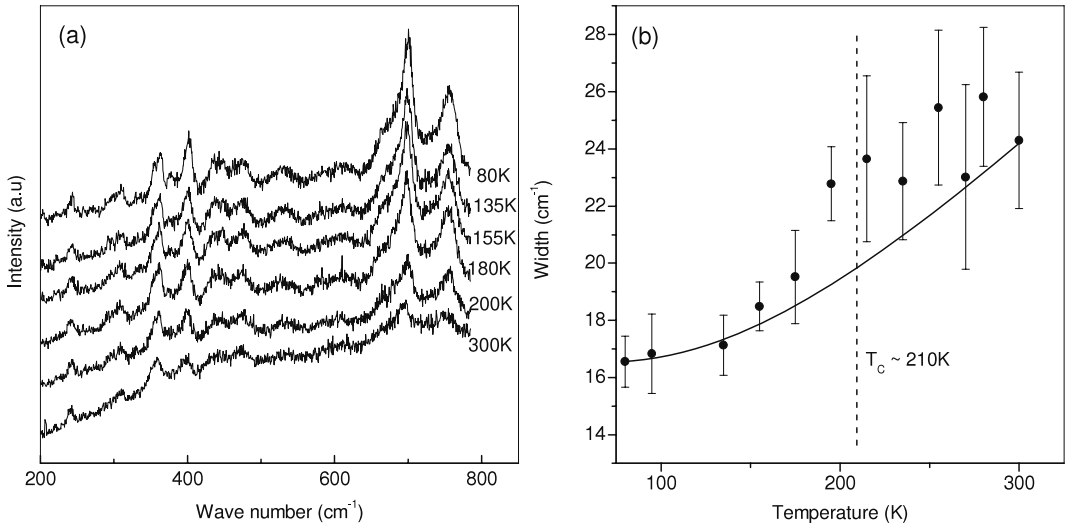

Figure 5. (a) Raman spectra measured in unpolarized geometry at some representative temperatures. (b) Variation of peak width as a function of temperature. The solid line in (b) is the simulation of equation (2). Note the anomaly around T_C.

Table 1. Hyperfine parameters with respect to natural iron obtained from the 5 K and 5 T ^{57}Fe Mossbauer data. IS, isomer shift; QS, quadrupole splitting; A23, area ratio of second and third lines in a sextet.

Site	FWHM (mm s^{-1})	IS (mm s^{-1})	QS (mm s^{-1})	H_{eff} (T)	A23	Area (%)	Moment (μ_B)	Weighted moment (μ_B)	χ^2
Fe1	0.49 ± 0.02	0.466 ± 0.007	-0.085 ± 0.02	54.92 ± 0.06	0.13 ± 0.04	31.2	3.787	1.182	1.38
Fe2	0.49 ± 0.02	0.488 ± 0.007	-0.16 ± 0.02	48.48 ± 0.05	0.76 ± 0.07	29.2	3.343	0.976	
A2	0.49 ± 0.02	0.478 ± 0.005	-0.196 ± 0.01	46.42 ± 0.08	1.66 ± 0.07	33.7	3.201	1.078	
A1	0.49 ± 0.02	0.312 ± 0.007	0.398 ± 0.02	43.17 ± 0.13	0.00	5.9	2.980	0.176	

lines of the sextet corresponding to site A1, i.e. a tetrahedral Ga1 site occupied by Fe, is constrained to be zero because of the fact that it is magnetically soft. The obtained hyperfine parameters with respect to natural iron at room temperature are shown in table 1. Isomer shift (IS) values give unambiguous information regarding the oxidation state and coordination number of iron. Fe^{2+} has a larger IS than Fe^{3+} and the IS is smaller for tetrahedral than octahedral coordination [18]. The observed IS of all sextets indicates the oxidation state of Fe^{3+} and the three sextets with relatively higher and the same IS values are assigned to three octahedral sites, namely Fe1, Fe2 and A2 sites, whereas the sextet of about 6% area with a smaller IS value is assigned to the tetrahedral A1 site. It may be noted that the MS of ε-Fe_2O_3, which is isomorphous with GFO, is fitted with four sextets corresponding to three octahedral Fe^{3+} sites and one tetrahedral Fe^{3+} site. The sextet corresponding to the tetrahedral Fe^{3+} site is identified with a relatively lower isomer shift and hyperfine field values [19], matching the present study. It may be noted that in the literature, using neutron diffraction and EXAFS measurements on single crystal samples which did not exhibit pinched-like M–H curve, population of Fe^{3+} is observed only at Fe1, Fe2 and A2 sites [4, 12]. Kim *et al*, observed the population of Fe at the A1 site in polycrystalline $AFeO_3$ (A = Ga and Al) samples from zero field Mossbauer data [20]. However, high field Mossbauer measurements not only give an unambiguous cation distribution but also information about the magnetic moment directions of different sites as discussed below.

The obtained effective hyperfine field (neglecting the demagnetizing field) is used to find the magnetic moment from the equation $H_{\text{eff}} = A\langle\mu_{\text{Fe}}\rangle$, where H_{eff} is the vector sum of the internal and external applied field and $A \approx 14.5$ T/μ_B [21]. The net magnetic moment is found to be $\sim$0.69 μ_B/Fe from the obtained relative population of Fe by considering that the moments of Fe1 and A1 sites point in the opposite direction to those of Fe2 and A2 sites, as shown in table 1, which closely matches the value of magnetization at 5 T (figure 3) justifying the fitting of the MS with four sextets. It may be noted that magnetic coupling between Fe atoms at the A1 site and at other sites is not explored in the literature because of the relatively small amount of Fe residing at the A1 site as compared to the A2 site. Therefore, the present study, which indicates that magnetic moments of Fe1 and A1 sites point in the opposite direction to those of Fe2 and A2 sites, assumes the significance.

Figure 5(a) shows the representative Raman spectra of GFO at the indicated temperatures. The measured data are corrected with Bose correction factor [22] to account for the temperature variation using the following equation, where I_{meas} is the measured intensity and T is temperature in kelvin:

$$I = I_{\text{meas}}\, T\, (1 - \exp(-1.439\,47/T)). \qquad (1)$$

Clear peaks corresponding to various Raman modes are observed. Vibrational modes (including Raman and IR active) of GFO, which consist of eight formula units i.e. 40 atoms in a unit cell, are calculated to be 120 modes, namely

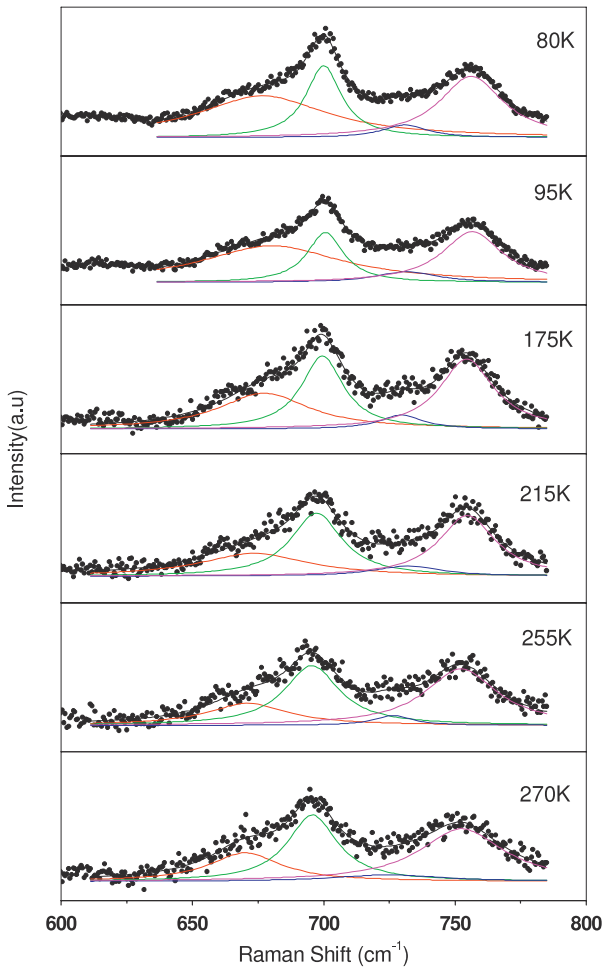

Figure 6. Representative Raman spectra at the indicated temperatures showing the detailed fitting.

$\Gamma_{Ga} = 6A_1 + 6A_2 + 6B_1 + 6B_2$, $\Gamma_{Fe} = 6A_1 + 6A_2 + 6B_1 + 6B_2$ and $\Gamma_O = 18A_1 + 18A_2 + 18B_1 + 18B_2$ [23]. We have attempted the polarized Raman measurements to distinguish various modes. But because of the polycrystalline nature of the sample, the changes in the intensity of modes in parallel and crossed polarization geometries is not the same as one would expect from polarization selection rules. It would be essential to do the polarized Raman measurements either on single crystal or epitaxial thin films to identify the nature of the modes. However, the conclusions drawn from the present Raman data as discussed below are considered to be significant for the understanding of role of phonons, and it has been shown that the Raman scattering from polycrystalline piezoelectric solids contains all of the essential features of Raman single crystal spectra [24].

One can clearly see from figure 5(a) that the overall Raman spectral signature is maintained across the ferrimagnetic–paramagnetic (fM–PM) transition. This is consistent with the fact that the fM–PM transition is not accompanied by any structural phase transition [4]. However, a closer inspection of the temperature dependent Raman spectra reveals interesting spectral changes in the vicinity of T_C. The evolution of the Raman spectra in the 600–800 cm^{-1} wavenumber region is deconvoluted into four peaks to obtain peak position and peak width at different temperatures. The detailed fitting of the representative data is shown as figure 6. The obtained variation of width of the peak at ∼700 cm^{-1} as a function of temperature is shown as figure 5(b). With increasing temperature the peak position is shifted to a lower wavenumber and broadens. This behavior is generally attributed to thermal expansion and thermal disorder, respectively. The temperature variation of peak width is theoretically simulated using a conventional formula [22] considering anharmonic coupling terms up to two phonons

$$\omega(T) = \omega_0 - C[1 + 2/(e^{\hbar\omega_0/kT} - 1)] \qquad (2)$$

where ω_0, C are adjustable parameters. The simulated curve is shown in figure 5(b) as a solid line. One can see the anomalous behavior of the variation of peak width at the magnetic transition temperature (T_C). This observation signifies the importance of the spin–phonon coupling in $GaFeO_3$. Recently, such anomalous behavior of phonons at the magnetic transition temperature is reported in the literature for multiferroic materials such as $BiFeO_3$, $YbMnO_3$ etc, signifying the importance of spin–phonon coupling in these materials for a better fundamental understanding of the phenomena [13, 14]. For example, in the case of rare-earth manganites such as $HoMnO_3$, $LuMnO_3$, $YbMnO_3$ etc, the importance of phonon effects using techniques like Raman, IR spectroscopy etc, is reported [13]. Apart from the rare-earth manganites, the other prominent multiferroic material, $BiFeO_3$, which crystallizes in a perovskite structure with space group $R3c$, has also been studied extensively using Raman spectroscopy in the context of spin–phonon coupling. Pronounced phonon anomalies around the magnetic transition temperature (T_N) are reported in the case of single crystals, epitaxial thin films and polycrystalline samples of $BiFeO_3$ [14]. However, calculation of allowed Raman active modes from group theory for GFO and their assignment to the observed peaks corresponding to various cation–oxygen bonds etc, are necessary to further comment on the observed results.

In conclusion, polycrystalline $GaFeO_3$ was prepared and studied using high field ^{57}Fe Mossbauer, magnetization and low temperature Raman measurements. The observed magnetic transition temperature (T_C) was 210 K. The multiferroic nature of the sample was evidenced from the observed anomaly at the T_C in the dielectric constant data. About 6% of the Fe population was observed at tetrahedral Ga1 sites from high field ^{57}Fe Mossbauer data, which explains the pinched-like behavior observed in the M–H curve. Comparison of the magnetization calculated from high field ^{57}Fe Mossbauer data and M–H data suggested that the Fe moment at Ga1 site is parallel to Fe1 and opposite to that of Fe2 and Ga2 sites resulting in ferrimagnetism. The Raman data of the $GaFeO_3$ are presented as a function of temperature from 80 to 300 K. It was observed that some phonons show anomalous behavior at T_C, indicating the importance of spin–phonon coupling in this material as in other multiferroic materials.

Acknowledgments

Authors thank DST, New Delhi for funding PPMS at CSR, Indore used for magnetization data in the present study.

DK thanks the Council of Scientific and Industrial Research (CSIR), India for a Senior Research Fellowship (SRF). Cryogenics, CSR is acknowledged for liquid helium.

References

[1] Khomskii D 2009 *Physics* **2** 20
Prellier W, Singh M P and Murugavel P 2005 *J. Phys.: Condens. Matter* **17** R803
Cheong S W and Mostovoy M 2007 *Nat. Mater.* **6** 13

[2] Yang C H, Koo T Y and Jeong Y H 2005 *Solid State Commun.* **134** 299

[3] Nowlin C H and Jones R V 1963 *J. Appl. Phys.* **34** 1262

[4] Arima T, Higashiyama D, Kaneko Y, He J P, Goto T, Miyasaka S, Kimura T, Oikawa K, Kamiyama T, Kumai R and Tokura Y 2006 *Phys. Rev.* B **70** 064426

[5] Remeika J P 1960 *J. Appl. Phys.* **31** 2635

[6] Abrahams S C and Reddy J M 1964 *Phys. Rev. Lett.* **13** 688
Abrahams S C, Reddy J M and Bernstein J L 1965 *J. Chem. Phys.* **42** 3957

[7] Han M J, Ozaki T and Yu J 2007 *Phys. Rev.* B **75** 060404(R)

[8] Frankel R B, Blum N A, Foner S, Freeman A J and Schieber M 1965 *Phys. Rev. Lett.* **15** 958

[9] Ogawa Y, Kaneko Y, He J P, Yu X Z, Arima T and Tokura Y 2004 *Phys. Rev. Lett.* **92** 047401

[10] Kubota M, Arima T, Kaneko Y, He J P, Yu X Z and Tokura Y 2004 *Phys. Rev. Lett.* **92** 137401

[11] Jung J H, Matubara M, Arima T, He J P, Kaneko Y and Tokura Y 2004 *Phys. Rev. Lett.* **93** 037403

[12] Kim J-Y, Koo T Y and Park J-H 2006 *Phys. Rev. Lett.* **96** 047205

[13] Souchkov A B *et al* 2003 *Phys. Rev. Lett.* **91** 027203
Litvinchuk A P *et al* 2004 *J. Phys.: Condens. Matter* **16** 809
Fukumura H, Hasuike N, Harima H, Kisoda K, Fukae K, Yoshimura T and Fujimura N 2009 *J. Phys.: Condens. Matter* **21** 064218

[14] Haumont R, Kreisel J, Bouvier P and Hippert F 2006 *Phys. Rev.* B **73** 132101
Ramirez M O, Krishnamurthi M, Denev S, Kumar A, Yang S-Y, Chu Y-H, Saiz E, Seidel J, Pyatakov A P, Bush A, Viehland D, Orenstein J, Ramesh R and Gopalan V 2008 *Appl. Phys, Lett.* **92** 022522
Rovillain P, Cazayous M, Gallais Y, Sacuto A, Lobo R P S M, Lebeugle D and Colson D 2009 *Phys. Rev.* B **79** 180411(R)

[15] Sun Z H, Cheng B L, Dai S, Cao L Z, Zhou Y L, Jin K J, Chen Z H and Yang G Z 2006 *J. Phys. D: Appl. Phys.* **39** 2481

[16] Naik V B and Mahendiran R 2009 *J. Appl. Phys.* **106** 123910

[17] Trooster J M and Dymanus A 1967 *Phys. Status Solidi* **24** 487

[18] Long G J and Grandjean F (ed) 1996 *Mossbauer Spectroscopy Applied to Magnetism and Materials Science* vol 2 (New York: Plenum) p 157

[19] Gich M, Frontera C, Roig A, Taboada E, Molins E, Rechenberg H R, Ardisson J D, Macedo W A A, Ritter C, Hardy V, Sort J, Skumryev V and Nogues J 2006 *Chem. Mater.* **18** 3889

[20] Kim W, We J H, Kim S J and Kim C S 2007 *J. Appl. Phys.* **101** 09M515

[21] Di N L, Cheng Z H, Li Q A, Wang G J, Kou Z Q, Ma X, Luo Z, Hu F X and Shen B G 2004 *Phys. Rev.* B **69** 224411

[22] Balkanski M, Wallis R F and Haro E 1983 *Phys. Rev.* B **28** 1928

[23] Fateley W G, McDevitt N T and Bentley F F 1971 *Appl. Spectrosc.* **25** 155

[24] Burns G and Scott B A 1970 *Phys. Rev. Lett.* **25** 1191